Scapular Motion Tracking Using Acromion Skin Marker Cluster: In Vitro Accuracy Assessment

Andrea Cereatti, Claudio Rosso, Ara Nazarian, Joseph P. DeAngelis, Arun J. Ramappa & Ugo Della Croce

Journal of Medical and Biological Engineering

ISSN 1609-0985

J. Med. Biol. Eng.
DOI 10.1007/s40846-015-0010-2

Springer

J. Med. Biol. Eng.
DOI 10.1007/s40846-015-0010-2

ORIGINAL ARTICLE

Scapular Motion Tracking Using Acromion Skin Marker Cluster: In Vitro Accuracy Assessment

Andrea Cereatti · Claudio Rosso · Ara Nazarian · Joseph P. DeAngelis · Arun J. Ramappa · Ugo Della Croce

Received: 11 October 2013 / Accepted: 20 March 2014

Abstract Several studies have recently investigated how the implementations of acromion marker clusters (AMCs) method and stereo-photogrammetry affect the estimates of scapula kinematics. However, in the large majority of these studies, the accuracy assessment of the scapular kinematics obtained with AMCs was carried out through a comparative evaluation using a scapula locator that is prone to error. The present study assesses AMC accuracy based on best practice recommendations, both with single and double anatomical calibration implementations, during several passive shoulder movements. Experiments were carried out on three cadaveric specimens. The scapula motion was acquired with a stereo-photogrammetric system using intra-cortical pins. When the scapula kinematics was estimated using an AMC combined with a single anatomical calibration, the accuracy was highly dependent on the specimen and the type of motion (maximum errors between –6.2° and 44.8°) and the scapular motion was generally overestimated. Moreover, with this implementation, scapular orientation errors increased for shoulder configurations distant from the reference shoulder configuration chosen for the calibration procedure. The double calibration implementation greatly improved the estimate of the scapular kinematics for all specimens and types of motion (maximum errors between –1.0° and 14.2°). The double anatomical calibration implementation should be preferred since it reduces the kinematics errors to levels which are acceptable in most clinical applications.

Keywords Acromion marker cluster · Scapular motion · Pitching · Throwing · Soft tissue artifacts

Andrea Cereatti and Claudio Rosso these authors have contributed equally to the work.

A. Cereatti · U. D. Croce
Information Engineering Unit, POLCOMING Department, University of Sassari, Sassari, Italy

A. Cereatti (✉)
Department of Information Engineering, Political Sciences and Communication Sciences, University of Sassari, Viale Mancini 5, 07100 Sassari, Italy
e-mail: acereatti@uniss.it

C. Rosso
Orthopaedic Department, University Hospital Basel, University of Basel, Basel, Switzerland

C. Rosso · A. Nazarian
Center for Advanced Orthopaedic Studies, Beth Israel Deaconess Medical Center and Harvard Medical School, Boston, MA, USA

J. P. DeAngelis · A. J. Ramappa
Department of Orthopaedic Surgery, Beth Israel Deaconess Medical Center, Harvard Medical School, Boston, MA, USA

1 Introduction

Non-invasive methods for measuring scapula motion are required in a variety of clinical and sports applications [1–6]. Tracking the acromion shows potential for estimating scapular movement. In the acromion method, either a magnetic sensor [7–12] or a photogrammetric marker cluster [13–18] is attached to the skin over the flat portion of the acromion, and scapula anatomical landmarks are calibrated with respect to a coordinate system fixed to the scapula. It has been shown that the acromion method accuracy is limited by the presence of soft tissue artifacts, especially when the full range of motion (ROM) of the gleno-humeral joint is explored [7, 8, 19, 20].

Recently, various studies have investigated several factors associated with the use of acromion marker clusters

Published online: 20 January 2015

(AMCs) and stereo-photogrammetry that may affect the overall accuracy: (a) the AMC design [13], (b) the shoulder posture selected for the scapula anatomical calibration [17], (c) the AMC attachment location [16], and d) the type of anatomical calibration (single or double) [15]. Moreover, AMC-based scapular motion has been compared to that obtained from skin-marker-based methods [14]. In most of AMC-based studies [13–17], the scapula kinematics, derived by manually pointing the anatomical landmarks by means of a specifically designed scapula locator during static measurements [21, 22], was used as reference for the assessment of the accuracy of the proposed method. However, it is generally agreed that quasi-static measurements combined with the use of the scapula locator are a "silver standard," since they are prone to errors caused by the anatomical landmark identification procedure and the presence of soft tissue artifacts [13, 15, 23].

The present study investigates the accuracy of the AMC-based method implemented according to the best practice recommendations proposed in recent studies [13, 16], both with single and double anatomical calibration implementations [15], using a reliable estimate of the actual motion of the bones of interest as a reference. Experiments were carried out using a cadaveric model and bone motion was recorded using AMCs mounted on intra-cortical pins and stereo-photogrammetry while different types of arm movement were generated by a robotic arm.

2 Materials and Methods

2.1 Specimens

Experiments were carried out on three fresh frozen specimens (the torso and both arms) from male donors (Medcure Anatomical Tissue Bank, Orlando, FL, USA). No detectable degenerative damage to the shoulder complex was present. The anthropometric characteristics of the three specimens are reported in Table 1.

2.2 Data Collection

Experimental data, consisting of the three-dimensional (3D) positions of reflecting markers in the global coordinate system, were acquired using a five-camera stereo-photogrammetric system (ProReflex Cameras, Qualisys, Gothenburg, Sweden) at 120 frames/s. The acquisition volume was a 1.5-m-sided cube.

The cadaver consisted of a whole torso from the lumbar spine level to the cervical spine level, including the rib cage. The muscles around the shoulder were all intact except for the inferior pelvic parts of the latissimus dorsi muscle. The soft tissues around the shoulder such as the skin and subcutaneous fat were left untouched for this study. The torso was mounted on a rod fixture attached to the fixed frame of the robotic system and held in place with volume-expanding foam (Fig. 1).

The radius and the ulna were attached to the moving frame of the robotic system using a Schanz pin. The moving frame was driven by controlled actuators and could move along three directions in space. Full descriptions of the robotic system and the experimental set-up can be found in previous works [24, 25].

While the specimen was secured to the robotic system, two steel pins (transosseous bi-cortical) were implanted into the humeral diaphysis and into the sternum, respectively. Each pin (6 mm in diameter) was equipped with a four-marker cluster separated by distances not shorter than 50 mm. For all tests, the skin was intact except for the stab incisions made for the positioning of the bone-embedded markers. An AMC, similar to that used by van Andel et al. [13], made of a light carbon frame and equipped with four markers (shortest distance between markers: 70 mm) was used to track the scapular motion. The AMC was made of a triangular base specifically shaped to be positioned over the flat part of the acromion close to the meeting point between the acromion and the scapular spine according to the guidelines proposed by Shaheen et al. [16] (Fig. 2). In order to identify the best AMC attachment location, the arm of the specimen was manually elevated and the AMC

Table 1 Humero-thorax angles for each shoulder motion and specimen (A, B, C) analyzed

Specimen	Type of motion	*Angle*	*Min* (°)	*Max* (°)	*ROM* (°)
A	Arm elev. sagittal pl.	β_h	51	145	94
	Arm elev. frontal pl.	β_h	95	146	52
	Abbr. throwing motion	γ_h	−37	−4	33
B	Arm elev. sagittal pl.	β_h	53	149	96
	Arm elev. frontal pl.	β_h	86	153	67
	Abbr. throwing motion	γ_h	−34	−1	33
C	Arm elev. sagittal pl.	β_h	71	152	80
	Arm elev. frontal pl.	β_h	108	163	55
	Abbr. throwing motion	γ_h	−32	−3	29

Minimal (*min*), maximal (*max*), and range of motion (*ROM*) values of humerus-thorax scalar rotation were estimated using humerus and thorax bone cluster

Fig. 1 Specimen A mounted on rod fixture, attached to fixed frame of robotic system, and held in place with volume-expanding foam

attachment was adjusted to minimize the interference with the anterior part of the deltoid muscle. The base of the AMC was made of deformable plastic and was attached using adhesive tape (triangle sides: 15, 15, and 20 mm) (Fig. 3). The total mass of the AMC was 0.0057 kg.

Before starting the dynamic data acquisition, while the arm was kept horizontally, the positions of the following anatomical landmarks [26] were measured using a pointer equipped with a four-marker cluster according to the *Calibration Anatomical System Techniques* (CAST) [27]: processus spinosus of the 7th cervical vertebra, processus spinosus of the 8th thoracic vertebra, deepest point of incisura jugularis, processus xiphoideus, most caudal point on lateral epicondyle, most caudal point on medial epicondyle and trigonum spinae scapulae, angulus inferior, angulus acromialis, most ventral point of processus, and most dorsal point on the acromioclavicular joint. The scapula anatomical landmarks were marked with an ink pen.

The following arm motions were generated by actuating programmed moving frame motions:

1. Arm elevation in the sagittal plane (starting horizontally).
2. Arm elevation in the frontal plane (starting horizontally).
3. Abbreviated throwing motion replicating the slow motion of the throwing of a professional pitcher from late cocking to early deceleration [28, 29] (starting horizontally).

Three repetitions of each type of motion were performed. The measurement of the scapular anatomical landmark positions was repeated for each type of motion, both at the initial and the final position of the arm according to the CAST [27].

Then, the AMC was replaced by an acromion bone-marker cluster (ABC), identical to the AMC except for the base, which was made of an alloy. The ABC was attached to the acromion using three screws (4 mm × 10 mm) (Fig. 2). While the arm was at the initial position, the locations of the scapular anatomical landmarks, previously marked, were recalibrated according to the CAST and the data collection procedure was repeated. The latter operation guaranteed for zero errors when comparing the scapular kinematics obtained using the AMC and the ABC at the beginning of arm motion.

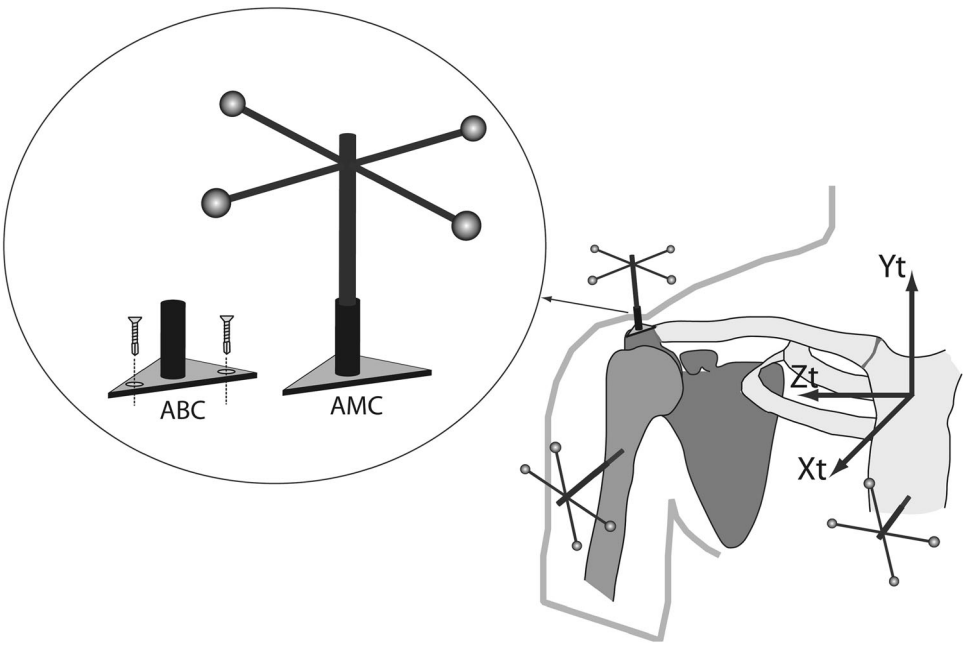

Fig. 2 Pin cluster and AMC configurations. A pin was drilled on the humeral diaphysis and into the sternum. Each cluster was made of four markers. The AMC was placed on the flat part of the acromion using adhesive tape. The ABC was attached to the acromion using three screws. The thorax coordinate system is depicted

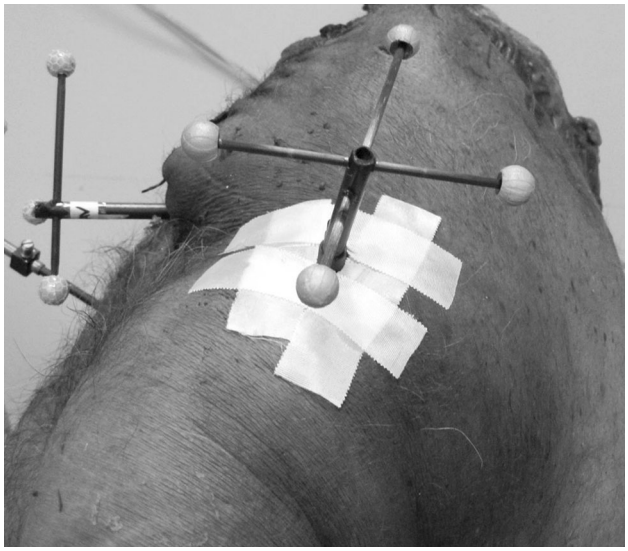

Fig. 3 AMC placed on the flat part of the acromion using adhesive tape

2.3 Data Processing

The poses of the marker cluster coordinate systems of the thorax, humerus, and scapula relative to the global coordinate system were estimated using a singular value decomposition technique [30]. The anatomical coordinate systems of the thorax, humerus, and scapula were defined according to the ISB recommendation [26] (Fig. 2) and were registered relative to the corresponding marker cluster coordinate systems. The location of the glenohumeral center was determined using regressive equations [31]. The orientations of the humerus and scapula relative to the thorax were described using the Euler angles in the Y–X–Y (α_h: plane of elevation, β_h: elevation, γ_h: axial rotation) and Y–X–Z sequences (α_s: protraction–retraction, β_s: lateral–medial rotation, γ_s: anterior–posterior tilt), respectively [26].

Marker position data recorded using the ABC were used to estimate the soft tissue artifact-free scapula kinematics, which served as the gold standard for evaluating the errors of the AMC-based estimate.

The AMC-based kinematics estimates were assessed both in single and double anatomical calibration implementations (AMC_1, AMC_2) [14, 32]. In the single anatomical calibration implementation, the anatomical landmarks of the scapula were registered with respect to the AMC at the starting arm position for each type of motion analyzed following the CAST [27]. In the double anatomical calibration implementation, the anatomical landmark registration was performed two times, namely at the start and end of arm motion.

The data reported by Karduna et al. [7] indicate that errors grow nonlinearly at the end range of humeral elevation. For this reason, to compensate for the soft tissue artifact effects, a nonlinear sinusoid weight function was adopted instead of previously proposed linear models [7, 15, 19]. In particular, the position vector $\mathbf{p}$ of each anatomical landmark in the AMC coordinate system was modeled through interpolation between the two calibration positions as a function of the corresponding humero-thoracic negative elevation β_h for arm motion in the sagittal and frontal planes:

$$\mathbf{p}(\beta_h) = \mathbf{p}_1 + (\mathbf{p}_2 - \mathbf{p}_1) \cdot 0.5 \cdot \left[1 - \sin\left(\frac{\beta_h - \beta_{h,1}}{\beta_{h,2} - \beta_{h,1}}\pi + \frac{\pi}{2}\right)\right] \quad (1)$$

where $\mathbf{p}_1$ and $\mathbf{p}_2$ are the scapular anatomical landmark position vectors identified during the anatomical calibrations performed at the beginning of the shoulder motion ($\beta_{h,1}$) and at the end ($\beta_{h,2}$), respectively. For the abbreviated throwing motion, the humero-thoracic axial rotation γ_h was used in Eq. 1 as an independent variable.

Having determined the anatomical landmark positions with respect to the relevant marker clusters, the kinematics of the scapula and humerus anatomical coordinate systems with respect to the thorax was estimated from the measured marker cluster trajectories during the analyzed motions. The scapular angular kinematics were then interpolated using cubic splines with the corresponding β_h rotation as an independent variable.

For each specimen and each type of motion, the interpolated data were averaged over the three trials recorded. The average over the ABC-based scapulo-thoracic kinematics estimate (α_s^{ABC}, β_s^{ABC}, γ_s^{ABC}) was used to assess the errors of the AMC-based estimate with single (α_s^{AMC1}, β_s^{AMC1}, γ_s^{AMC1}) and double anatomical calibration implementations (α_s^{AMC2}, β_s^{AMC2}, γ_s^{AMC2}). For each subject and type of motion, the following quantities were computed: the scapular angular kinematics error $\mathbf{e} = \begin{bmatrix} e_\alpha \\ e_\beta \\ e_\gamma \end{bmatrix} = \begin{bmatrix} \alpha_s^{AMC} - \alpha_s^{ABC} \\ \beta_s^{AMC} - \beta_s^{ABC} \\ \gamma_s^{AMC} - \gamma_s^{ABC} \end{bmatrix}$ associated with both single and double anatomical calibrations; the maximum scapula angular error over the shoulder motion ($\boldsymbol{e}_{max}$), the mean absolute scapula angular error over the shoulder motion ($|\boldsymbol{e}|$), and the scapula angular ROM errors ($\boldsymbol{e}_{ROM}$).

The repeatability of the robotic-system-generated scapula movements was assessed for all specimens and types of motion by computing the average of the standard deviation values of the scapular kinematics (α_s, β_s, γ_s) over the three trials, estimated using both the AMC and the ABC.

3 Results

The thoraco-humeral ROM generated by the robotic system differed for the three specimens (Table 1) due to their different anthropometries (Table 2).

The average standard deviation values of α_s, β_s, and γ_s computed over the three movement repetitions for both the AMC and the ABC varied for all motions between 0.1° and 0.4°. The scapular-thorax angular error components obtained for AMC_1 and AMC_2 for the different arm motions for the three specimens are shown in Figs. 4, 5, and 6, respectively.

3.1 Single Anatomical Calibration

The largest errors were observed for specimen A ($\mathbf{e}_{max}$ up to –44.8° for β_s), followed by specimen B ($\mathbf{e}_{max}$ up to –14.9° for β_s) and specimen C ($\mathbf{e}_{max}$ up to –6.2° along α_s) (Table 3; Figs. 4a, 5a, and 6a). During the arm motion in the sagittal plane, the scapula angular ranges of motion were overestimated for all specimens and components (Table 3). During the arm motion in the frontal plane, specimen A showed large errors ($\mathbf{e}_{max}$ up to 38.9° for β_s), with the maximum errors for subjects B and C being limited for all components ($\mathbf{e}_{max}$ up to –9.3° and 5.7° for γ_s, respectively). During the abbreviated throwing motion, errors exhibited smaller variations throughout the motion and across specimens. The largest errors were observed for specimen B ($\mathbf{e}_{max}$ up to 12.7° along γ_s). For all specimens and types of motion, errors tended to increase at the end of the recorded movement (Figs. 4a, 5a, 6a).

3.2 Double Anatomical Calibration

An overall reduction of the $\boldsymbol{e}_{ROM}$, $\boldsymbol{e}_{max}$, and $\boldsymbol{e}_{ma}$ values was observed for all specimens and types of motion with double anatomical calibration (Fig. 4b, 5b, 6b). During the arm motion in the sagittal plane, specimen A showed the largest errors ($\mathbf{e}_{max}$ up to 14.2° along β_s), with the maximum errors for subjects B and C being limited for all components (<6.3°) (Table 4). During the arm motion in the frontal plane, the $\mathbf{e}_{max}$ component values ranged from 1.2° to –7.5° across specimens and types of motion. During the abbreviated throwing motion, the $\mathbf{e}_{max}$ component values ranged from –1.0° to 4.6° across specimens and types of motion. A general scapula angular ROM overestimation was observed for all specimens and types of motion (Table 4).

Table 2 Anthropometric characteristics of specimens

Specimen	Sex	Age	Height (m)	Mass (kg)	BMI (kg/m^2)
A	Male	57	1.83	139	40.3
B	Male	67	1.78	84	26.5
C	Male	50	1.54	53	22.3

4 Discussion

In the present paper, the accuracy of the scapular kinematics obtained using the AMC with single and double anatomical calibrations was assessed in vitro. The arm movement was passively driven using a robotic system, which allowed different types of motion to be generated in a highly repeatable manner, as demonstrated by the negligible differences observed in scapular motion among the corresponding trial repetitions (SD < 0.4°) [24]. Given the truly passive condition, the scapulathoracic motion observed was therefore controlled by the capsuloligamentous and passive muscle tension during arm elevation [33].

The adoption of a robotic apparatus combined with a cadaveric model allowed the soft tissue artifact effects on scapula kinematics estimated using the AMC during passive shoulder movement to be assessed. An important limitation associated with the use of an in vitro model is that the soft tissue artifacts are only due to skin stretching in the proximity of the joint and to passive muscle stretching and bulging. However, this approach may offer some advantages over non-invasive in vivo approaches. First, scapular kinematics was analyzed during continuous shoulder movements instead of an ensemble of quasi-static configurations [8, 13–17]. Second, the scapula motion provided by the ABC allowed for the direct tracking of scapular motion and therefore can be considered a highly reliable gold standard. Conversely, the use of a scapula locator employed in previous studies aimed at assessing the AMC method accuracy requires the manual identification of the 3D scapula orientation by means of anatomical landmark identification. The latter operation is associated with errors [13] and may affect the scapula kinematics [34].

Due to the unavoidable deformation of the soft tissues surrounding the scapula, during shoulder motions, the AMC moves with respect to the underlying bone, and therefore the scapula anatomical landmark positions relative to the AMC coordinate systems vary with respect to their reference positions acquired during the calibration. The scapular orientation errors are thus expected to increase for shoulder configurations distant from the reference shoulder configuration chosen for the calibration procedure [17]. Several previous studies performed a single anatomical calibration while the subject kept the arm vertically along the body [7, 13, 15], concluding that the acromion method was less accurate for higher degrees of humerus elevation. As noted by Prinold et al. [17], the large errors observed (>100°) are mainly related to the

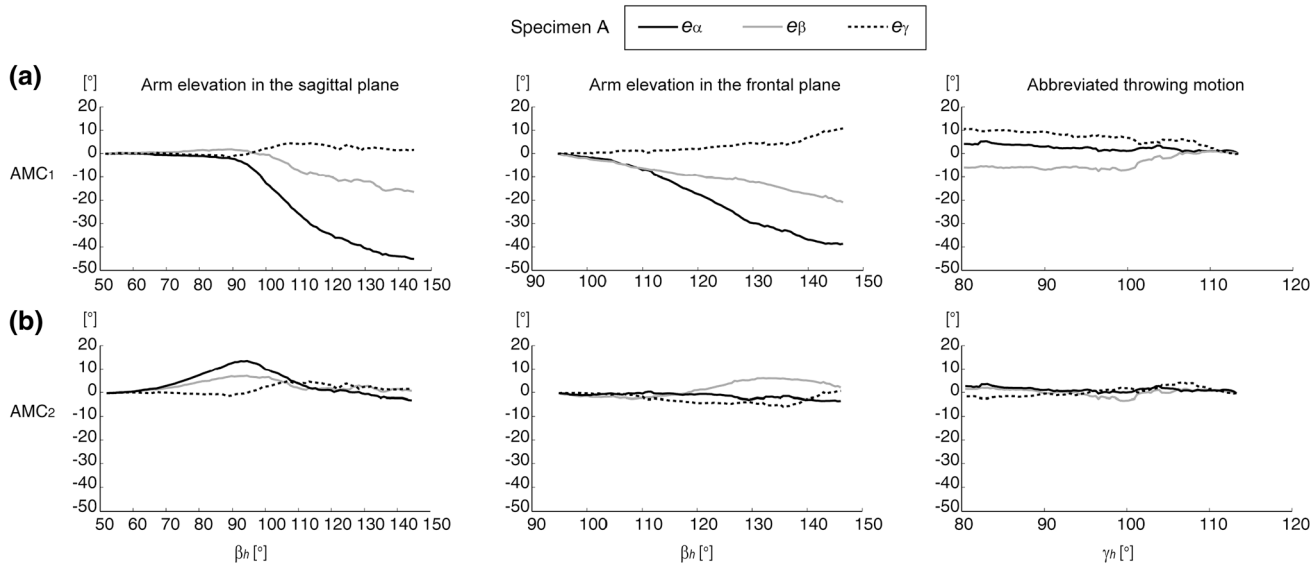

Fig. 4 Scapula-thorax angular error components (e_α protraction–retraction, e_β lateral–medial rotation, e_γ anterior–posterior tilt) estimated for specimen A with **a** single and **b** double calibration implementations expressed as function of humerus-thorax rotation (β_h elevation, γ_h axial rotation) for the different motions. All values are expressed in degrees

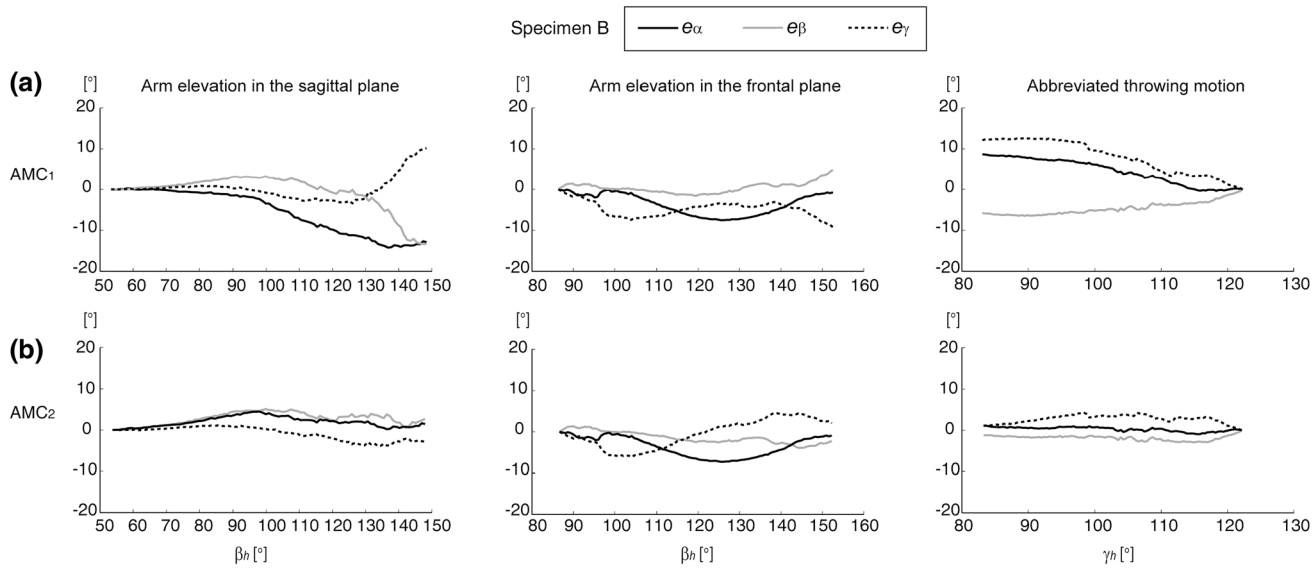

Fig. 5 Scapula-thorax angular error components (e_α protraction–retraction, e_β lateral–medial rotation, e_γ anterior–posterior tilt) estimated for specimen B for **a** single and **b** double calibration implementations expressed as function of humerus-thorax rotation (β_h elevation, γ_h axial rotation) for the different motions. All values are expressed in degrees

specific shoulder configuration selected for the anatomical calibration.

When the scapula kinematics was estimated using the AMC combined with a single anatomical calibration, the results suggest that the accuracy level is highly dependent on the specimen and type of motion. Maximum errors varied between –6.2° for specimen C [body mass index (BMI) = 21.9] and 44.8° for specimen A (BMI = 40.3). In this regard, it is worth noticing that the three specimens presented substantial anthropometric differences in terms of height, mass, and muscle volume, which resulted in different amounts of soft tissue artifacts [15]. The largest errors were found in the estimates of lateral/medial scapular rotation during the humeral elevation in the sagittal plane. The large errors found for specimen A (obese) can be explained by the presence of a large deformation of the soft tissue covering the bone. However, it is worthwhile noting that the mean absolute error affecting the lateral/

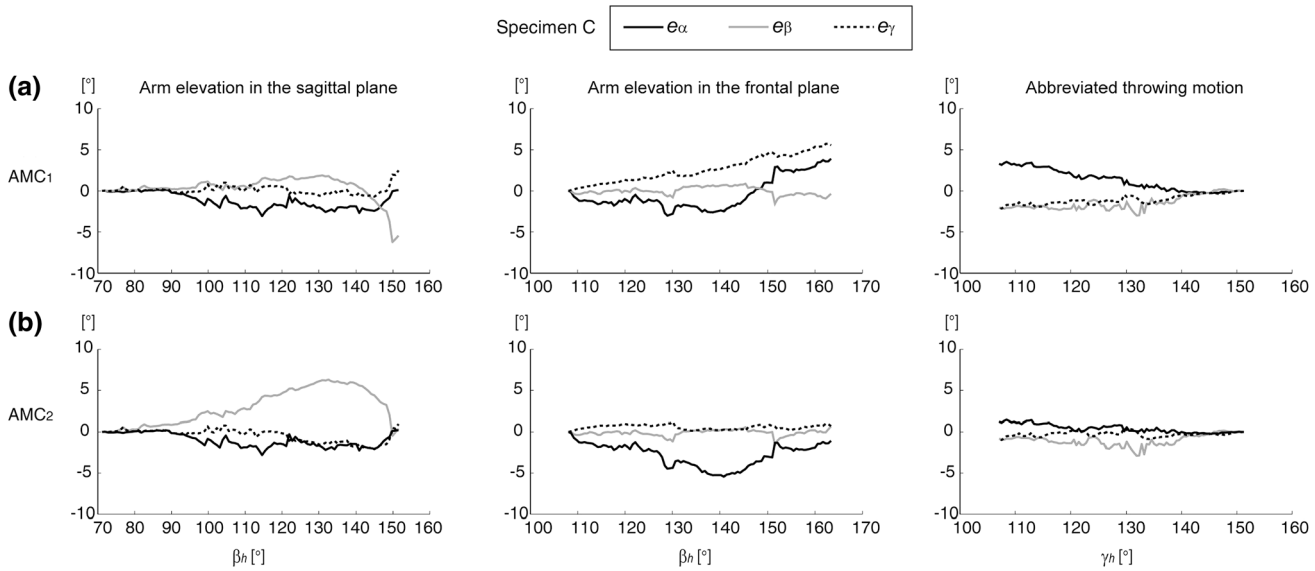

Fig. 6 Scapula-thorax angular error components (e_α protraction–retraction, e_β lateral–medial rotation, e_γ anterior–posterior tilt) estimated for specimen C for **a** single and **b** double calibration implementations expressed as function of humerus-thorax rotation (β_h elevation, γ_h axial rotation) for the different motions. All values are expressed in degrees

Table 3 Assessment of scapula-thorax angular estimates obtained using AMC with single anatomical calibration implementation

			$\boldsymbol{ROM}_{ABC}$ (°)			$\boldsymbol{e}_{ROM}$ (°)			$\boldsymbol{e}_{max}$ (°)			$\lvert\boldsymbol{e}\rvert$ (°)		
		Motion	α_s	β_s	γ_s	α_s	β_s	γ_s	α_s	β_s	γ_s	α_s	β_s	γ_s
Specimen	A	Arm elev. sagittal pl.	13.1	36.2	20.3	17.2	43.7	2.1	−16.9	−44.8	4.5	4.8	17.1	1.6
		Arm elev. frontal pl.	2.4	27.0	12.9	16.9	37.2	10.7	−20.7	−38.9	11.1	9.5	18.2	2.9
		Abbr. throwing motion	24.2	22.5	5.8	−5.9	4.2	−0.2	−7.4	5.4	10.7	4.3	2.5	6.9
	B	Arm elev. sagittal pl.	22.2	42.9	24.7	16.4	12.9	10.2	−13.4	−14.3	10.2	2.8	5.6	1.9
		Arm elev. frontal pl.	7.8	40.7	33.3	−0.3	0.7	−9.3	4.9	−7.6	−9.3	1.0	3.6	4.8
		Abbr. throwing motion	34.7	23.0	6.3	−5.8	8.7	1.5	−6.5	8.7	12.7	4.6	4.5	8.0
	C	Arm elev. sagittal pl.	8.9	46.4	18.9	6.6	−0.1	1.8	−6.2	−3.1	2.5	1.0	1.2	0.4
		Arm elev. frontal pl.	14.4	45.4	17.6	0.6	−3.9	5.5	−1.6	3.9	5.7	0.4	1.8	2.6
		Abbr. throwing motion	41.4	23.9	3.5	−2.1	3.3	2.0	−3.0	3.5	−2.1	1.5	1.4	1.1

For each shoulder motion and specimen analyzed (A, B, C), the accuracy of the scapula angular component (protraction/retraction α_s, lateral/medial rotation β_s, and anterior/posterior tilt γ_s) estimates obtained using AMC_1 were assessed using ABC estimates as the gold standard. $\boldsymbol{ROM}_{ABC}$ ROM estimated using ABC, $\boldsymbol{e}_{ROM}$ overestimation (+)/underestimation (−) error of the scapula angular ROM, $\boldsymbol{e}_{max}$ maximum scapula angular error, $\lvert\boldsymbol{e}\rvert$ mean absolute scapula angular error over the shoulder motion

medial scapular rotation, averaged over the three specimens analyzed (about 8°), is comparable to the average root-mean-square error value (5.9°) found by Karduna et al. [7] during the humerus elevation. A general tendency toward an overestimation of the scapula ROMs was observed for all specimens and types of motion. It was particularly evident for the arm motion in the sagittal plane. Among the shoulder motions analyzed, the smallest errors were found in the abbreviated throwing motion ($\mathbf{e}_{max}$ components <11° across specimens). These results might support the use of AMC_1 for the scapular recording during shoulder movements involving a small variation of the humerus elevation angle.

The double calibration improved the scapula kinematics estimates for all subjects and types of motion. The high error variability across specimens found using AMC_1 was greatly reduced. The maximum errors varied between −3.2° and 14.2° for specimen A, between 1.2° and −7.5° for specimen B, and between −1.0° and 6.3° for specimen C. The patterns of the scapula kinematics components were well reproduced for all subjects and types of motion and the accuracy ($\lvert\boldsymbol{e}\rvert$ component values between 0.3° and 4.7°) was similar to that found in previous studies based on the use of a scapula locator [15, 19]. The ROM estimation errors varied across subjects and types of motion between −0.1° and 5.5°, except for the lateral-medial rotation in

Table 4 Assessment of scapula-thorax angular estimates obtained using AMC with double anatomical calibration implementation

			e_{ROM} (°)			e_{max} (°)			|e| (°)		
		Motion	α_s	β_s	γ_s	α_s	β_s	γ_s	α_s	β_s	γ_s
Specimen	A	Arm elev. sagittal pl.	5.5	12.8	2.0	7.6	14.2	5.2	3.2	4.7	1.8
		Arm elev. frontal pl.	5.2	3.2	1.0	6.5	−3.3	−5.7	3.0	1.2	2.5
		Abbr. throwing motion	1.9	3.1	3.6	−3.2	4.0	4.6	1.3	1.6	1.6
	B	Arm elev. sagittal pl.	2.4	−1.1	−2.8	5.2	4.6	−4.0	2.9	2.0	1.4
		Arm elev. frontal pl.	1.6	0.9	2.2	−4.0	−7.5	−6.3	1.7	3.7	3.1
		Abbr. throwing motion	−1.2	1.2	1.7	−3.0	1.2	4.4	1.9	0.5	2.8
	C	Arm elev. sagittal pl.	5.5	−0.2	0.3	6.3	−2.8	−2.1	3.0	1.1	0.6
		Arm elev. frontal pl.	−0.1	1.1	0.7	−1.6	−5.4	1.2	0.3	2.8	0.6
		Abbr. throwing motion	−0.8	1.2	0.9	−2.9	1.4	−1.0	1.0	0.5	0.3

For each shoulder motion and specimen analyzed (A, B, C), the accuracy of the scapula angular component (protraction/retraction α_s, lateral/medial rotation β_s, and anterior/posterior tilt γ_s) estimates obtained using AMC_2 were assessed using ABC estimates as the gold standard. $\boldsymbol{ROM}_{ABC}$ ROM estimated using ABC, $\boldsymbol{e}_{ROM}$ overestimation (+)/underestimation (−) error of the scapula angular ROM, $\boldsymbol{e}_{max}$ maximum scapula angular error, $|\boldsymbol{e}|$ mean absolute scapula angular error over the shoulder motion

specimen A, which exhibited an overestimation of up to 12.8°. The residual kinematics errors observed at the end of the motion are associated with the uncertainty in the identification of the anatomical landmarks [35].

It is important to acknowledge that the sinusoidal weight function used for AMC_2 was symmetric with respect to the midpoint of the humerus elevation ROM, and hence the results of the double calibration procedure were independent of the order of the shoulder configurations selected for the anatomical landmark calibration. When the experimentally measured soft tissue artifacts were in good accordance with the model, as observed in specimen A during the arm motion in the frontal plane, the use of the double calibration approach was extremely effective, with the maximum errors found using AMC_1 highly reduced using AMC_2 (from −20.7° to 6.5°, from −38.9° to −3.3°, and from 11.1° to −5.7° for protraction–retraction, lateral–medial rotation, and anterior–posterior tilt, respectively). Conversely, in specimen A, during the arm motion in the sagittal plane, anatomical landmark displacement with respect to the AMC coordinate system were negligible, from 50° (initial calibration) to 90° for humeral elevation and then increasing to 90°–145° (final calibration) (Fig. 4b). In this specific case, the errors affecting the scapula-thorax orientation estimates are highly asymmetric and could not be corrected by the symmetric model. Therefore, at about 90° of shoulder elevation, the double calibration method performed slightly worse than the single anatomical calibration. If required for specific clinical needs, a further reduction of the kinematics errors could be obtained by performing an additional anatomical calibration at the midpoint of the arm motion [19].

The results found in this study should be interpreted in light of inherent limitations and caution is required when comparing them with those reported in in vivo studies. The use of a cadaveric model means that the soft tissue artifacts affecting the scapula tracking differed from those that may be observed during active movements mainly because of the absence of muscular contraction, such as that of the deltoid [13]. The AMC accuracy assessment carried out in this study can thus be considered suitable when passive shoulder movements with no or negligible muscle activity are analyzed [36]. Additionally, the thawing process may have caused differences in the tissue viscoelasticity with respect to the living counterpart [37]. Moreover, due to the robotic apparatus constraints, the arm starting position at the beginning of the sagittal and frontal motions was in general more elevated with respect to those in previous studies [7, 8, 15, 17] and therefore the ROMs analyzed were in general smaller. However, despite the relatively smaller humerothoracic ROM, the scapular angular displacements measured using the ABC were large and comparable to those found using invasive bone markers in vivo [4] (medial/lateral rotation varied across subjects, between 36° and 46° during the arm elevation in the sagittal plane and between 27° to 45° during the arm elevation in the frontal plane). Lastly, the limited number of specimens (three) analyzed precluded statistical analysis from being performed and thus comparisons with results from previous studies should be done cautiously. However, the highly repeatable measurements carried out using the innovative experimental setup and appropriate methodology provide results characterized by an extremely high reliability. Unfortunately, given the consequent high cost of the experiments, a larger dataset is not foreseeable in the near future.

5 Conclusion

In conclusion, under passive conditions, the accuracy of the AMC method with the single anatomical calibration

implementation was highly variable across specimens and types of motion, and reliable within a limited shoulder ROM close to the calibration configuration. The implementation of the double anatomical calibration should be preferred since it allowed a reduction of scapula kinematics errors within levels acceptable in most clinical applications. However, in some cases, the soft tissue artifact correction might be not equally effective over the full shoulder ROM.

Acknowledgments The authors would like to acknowledge the Medical Advisory Committee for Major League Baseball (AJR and AN) and the Department of Orthopaedic Surgery at Beth Israel Deaconess Medical Center, Boston, MA (AN and AJR) for funding this project. They would like to gratefully acknowledge the Swiss National Science Foundation for providing funding to Drs. Claudio Rosso for his work on this project.

References

1. Myers, J. B., Laudner, K. G., Pasquale, M. R., Bradley, J. P., & Lephart, S. M. (2005). Scapular position and orientation in throwing athletes. *The American Journal of Sports Medicine, 33*, 263–271.
2. Forthomme, B., Crielaard, J. M., & Croisier, J. L. (2008). Scapular positioning in athlete's shoulder: Particularities, clinical measurements and implications. *Sports Medicine (Auckland, N. Z.), 38*, 369–386.
3. Miyashita, K., Kobayashi, H., Koshida, S., & Urabe, Y. (2010). Glenohumeral, scapular, and thoracic angles at maximum shoulder external rotation in throwing. *The American Journal of Sports Medicine, 38*, 363–368.
4. Ludewig, P. M., Phadke, V., Braman, J. P., Hassett, D. R., Cieminski, C. J., & LaPrade, R. F. (2009). Motion of the shoulder complex during multiplanar humeral elevation. *The Journal of Bone and Joint Surgery, 91*, 378–389.
5. Hill, A. M., Bull, A. M., Dallalana, R. J., Wallace, A. L., & Johnson, G. R. (2007). Glenohumeral motion: Review of measurement techniques. *Knee Surgery, Sports Traumatology, Arthroscopy, 15*, 1137–1143.
6. Anglin, C., & Wyss, U. P. (2000). Review of arm motion analyses. *Proceedings of the Institution of Mechanical Engineers, Part H, 214*, 541–555.
7. Karduna, A. R., McClure, P. W., Michener, L. A., & Sennett, B. (2000). Dynamic measurements of three-dimensional scapular kinematics: A validation study. *Journal of Biomechanical Engineering, 123*, 184–190.
8. Meskers, C. G., van de Sande, M. A., & de Groot, J. H. (2007). Comparison between tripod and skin-fixed recording of scapular motion. *Journal of Biomechanics, 40*, 941–946.
9. Fayad, F., Hoffmann, G., Hanneton, S., Yazbeck, C., Lefevre-Colau, M. M., Poiraudeau, S., et al. (2006). 3-D scapular kinematics during arm elevation: Effect of motion velocity. *Clinical Biomechanics, 21*, 932–941.
10. Fayad, F., Roby-Brami, A., Yazbeck, C., Hanneton, S., Lefevre-Colau, M. M., Gautheron, V., et al. (2008). Three-dimensional scapular kinematics and scapulohumeral rhythm in patients with glenohumeral osteoarthritis or frozen shoulder. *Journal of Biomechanics, 4*, 326–332.
11. McQuade, K. J., & Smidt, G. L. J. (1998). Dynamic scapulohumeral rhythm: The effects of external resistance during elevation of the arm in the scapular plane. *Journal of Orthopaedic and Sports Physical Therapy, 27*, 125–133.
12. McCully, S. P., Kumar, N., Lazarus, M. D., & Karduna, A. R. (2005). Internal and external rotation of the shoulder: Effects of plane, end-range determination, and scapular motion. *Journal of Shoulder and Elbow Surgery, 14*, 602–610.
13. van Andel, C., van Hutten, K., Eversdijk, M., Veeger, D., & Harlaar, J. (2009). Recording scapular motion using an acromion marker cluster. *Gait and Posture, 29*, 123–128.
14. Brochard, S., Lempereur, M., & Remy-Neris, O. (2011). Accuracy and reliability of three methods of recording scapular motion using reflective skin markers. *Proceedings of the Institution of Mechanical Engineers, Part H, 225*, 100–105.
15. Brochard, S., Lempereur, M., & Rémy-Néris, O. (2011). Double calibration: An accurate, reliable and easy-to-use method for 3D scapular motion analysis. *Journal of Biomechanics, 44*, 751–754.
16. Shaheen, F., Alexander, C. M., & Bull, A. M. (2011). Effects of attachment position and shoulder orientation during calibration on the accuracy of the acromial tracker. *Journal of Biomechanics, 44*, 1410–1413.
17. Prinold, J. A., Shaheen, A. F., & Bull, A. M. (2011). Skin-fixed scapula trackers: A comparison of two dynamic methods across a range of calibration positions. *Journal of Biomechanics, 44*, 2004–2007.
18. Warner, M. B., Chappell, P. H., & Stokes, M. J. (2012). Measuring scapular kinematics during arm lowering using the acromion marker cluster. *Human Movement Science, 31*, 386–396.
19. Bourne, D. A., Choo, A. M., Regan, W. D., Macintyre, D. L., & Oxland, T. R. (2009). A new subject-specific skin correction factor for three-dimensional kinematic analysis of the scapula. *Journal of Biomechanical Engineering-T ASME, 131*, 121009.
20. Bourne, D. A., Choo, A. M., Regan, W. D., MacIntyre, D. L., & Oxland, T. R. (2011). The placement of skin surface markers for non invasive measurement of scapular kinematics affects accuracy and reliability. *Annals of Biomedical Engineering, 39*, 777–785.
21. Johnson, G. R., Stuart, P. R., & Mitchell, S. (1993). A method for the measurement of 3-dimensional scapular movement. *Clinical Biomechanics, 8*, 269–273.
22. Barnett, N. D., Duncan, R. D., & Johnson, G. R. (1999). The measurement of three dimensional scapulohumeral kinematics-a study of reliability. *Clinical Biomechanics, 14*, 287–290.
23. Cutti, A. G., & Veeger, H. E. (2009). Shoulder biomechanics: Today's consensus and tomorrow's perspectives. *Medical and Biological Engineering and Computing, 47*, 463–466.
24. Entezari, V., Trechsel, B. L., Dow, W. A., Stanton, S. K., Rosso, C., Müller, A., et al. (2012). Design and manufacture of a novel system to simulate the biomechanics of basic and pitching shoulder motion using a cadaveric model. *Bone and Joint Research, 1*, 78–85.
25. Rosso, C., Müller, A. M., Entezari, V., Dow, W. A., McKenzie, B., Stanton, S. K., et al. (2013). Preliminary evaluation of a robotic apparatus for the analysis of passive glenohumeral joint kinematics. *Journal of Orthopaedic Surgery and Research, 8*, 24.
26. Wu, G., van der Helm, F. C., Veeger, H. E., Makhsous, M., Van Roy, P., Anglin, C., et al. (2005). ISB recommendation on definitions of joint coordinate systems of various joints for the reporting of human joint motion-part II: Shoulder, elbow, wrist and hand. *Journal of Biomechanics, 38*, 981–992.
27. Cappozzo, A., Catani, F., Della Croce, U., & Leardini, A. (1995). Position and orientation of bones during movement: Anatomical frame definition and determination. *Clinical Biomechanics, 10*, 171–178.
28. Meister, K. (2000). Injuries to the shoulder in the throwing athlete. Part one: Biomechanics/pathophysiology/classification of injury. *The American Journal of Sports Medicine, 28*, 265–275.
29. Mueller, A. M., Entezari, V., Rosso, C., McKenzie, B., Hasebrock, A., Cereatti, A., et al. (2013). The effect of simulated

scapular winging on glenohumeral joint translations. *Journal of Shoulder and Elbow Surgery, 22*, 986−992.
30. Soderkvist, I., & Wedin, P. A. (1993). Determining the movements of the skeleton using well-configured markers. *Journal of Biomechanics, 26*, 1473–1477.
31. Meskers, C. G., van der Helm, F. C., & Rozendaal, L. A. (1998). In vivo estimation of the glenohumeral joint rotation center from scapular bony landmarks by linear regression. *Journal of Biomechanics, 31*, 93–96.
32. Cappello, A., Cappozzo, A., La Palambora, P. F., Lucchetti, L., & Leardini, A. (1997). Multiple anatomical landmark calibration for optimal bone pose estimation. *Human Movement Science, 16*, 259–274.
33. Price, C. I., Franklin, P., Rodgers, H., Curless, R. H., & Johnson, G. R. (2000). Active and passive scapulohumeral movement in healthy persons: A comparison. *Archives of Physical Medicine and Rehabilitation, 81*, 28–31.
34. Shaheen, A. F., Alexander, C. M., & Bull, A. M. (2001). Tracking the scapula locator with and without feedback from pressure-sensors: A comparative study. *Journal of Biomechanics, 44*, 1633–1636.
35. Della Croce, U., Cappozzo, A., & Kerrigan, D. C. (1999). Pelvis and lower limb anatomical landmark calibration precision and its propagation to bone geometry and joint angles. *Medical and Biological Engineering and Computing, 37*, 155–161.
36. Ebaugh, D. D., McClure, P. W., & Karduna, A. R. (2005). Three-dimensional scapulothoracic motion during active and passive arm elevation. *Clinical Biomechanics, 20*, 700–709.
37. Veronda, D. R., & Westmann, R. A. (1970). Mechanical characterization of skin-finite deformations. *Journal of Biomechanics, 31*, 111–124.